DTU Library

Class D audio amplifier with 4th order output filter and self-oscillating full-state hysteresis based feedback driving capacitive transducers

Nielsen, Dennis; Knott, Arnold; Andersen, Michael A. E.

Published in:
Proceedings of EPE'14-ECCE

Link to article, DOI:
10.1109/EPE.2014.6910924

Publication date:
2014

Document Version
Peer reviewed version

Class D audio amplifier with 4th order output filter and self-oscillating full-state hysteresis based feedback driving capacitive transducers

Dennis Nielsen, Arnold Knott & Michael A. E. Andersen
Technical University of Denmark
Oersteds Plads, Building 349
Dk-2800 Kgs. Lyngby, Denmark
Phone: +45 45253490
Fax: +45 45880117
Email: deni@elektro.dtu.dk
URL: http://www.elektro.dtu.dk

Keywords

Sliding mode control, High voltage power converters, Drive, Active damping, Amplifiers

Abstract

A practical solution is presented for the design of a non-isolated high voltage DC/AC power converter. The converter is intended to be used as a class D audio amplifier for a Dielectric Electro Active Polymer (DEAP) transducer. A simple and effective hysteretic control scheme for the converter (buck with fourth-order output filter) is developed and analyzed. The proposed design is verified experimentally by a 125 VAR prototype amplifier, capable of delivering a peak output voltage of 240 V within the frequency range of 100 Hz – 3.5 kHz. A peak efficiency of 87 % is reported.

Introduction:

Sound reproduction systems are commonly build around class D audio amplifiers due to their superior cost, size and efficiency compared to their linear counterparts [1, 2, 3, 4, 5]. While these audio systems are dominating the market of sound reproduction, they still suffer from the poor efficiency imposed by the electrodynamic transducer. An alternative to the electrodynamic transducer is the capacitive transducer. Capacitive transducers are most known from their usage in electrostatic loudspeakers, however Dielectric Electro Active Polymers (DEAP) can also be used to form a capacitive transducer [6, 7, 8]. With the goal of creating smaller, cheaper and more efficient audio systems it is proposed to use a class D amplifier as driver of the capacitive transducer [9, 10]. Class D amplifiers driving a capacitive transducer without the use of audio or high frequency linked transformers, is an area of research with little to no publications. This paper addresses the issue of limited frequency response and high series resistance of capacitive transducers. The focus of the paper is placed upon Dielectric Electro Active Polymer (DEAP) transducers, however the concept can easily be extended to other capacitive transducers like piezoelectric ones.

A push DEAP transducer is shown in figure 1, while the measured impedance of the transducer is presented in figure 2. It is observed from figure 2, that the transducer cannot be expected to act as a capacitor for frequencies above 100 kHz. This limits the switching frequency significantly, if the output filter is constructed entirely by an inductor and the DEAP. Film or ceramic capacitors could be placed in parallel with the DEAP transducer. This will improve the frequency response. However it will also increase the reactive output power of the amplifier, because the capacitive load is increased. Another concern of the DEAP transducer is the series resistance. Older versions of the DEAP material [6] exhibited series resistance up to 50 Ω, while the present versions are specified within the region of 1–10 Ω. The connection between the DEAP transducer and the surrounding electronics is even more complicated than that of the film capacitor. DEAP transducers are constructed by printing compliant electrodes on a silicone membrane. The contact is performed on a surface exposed to significant mechanical stress.

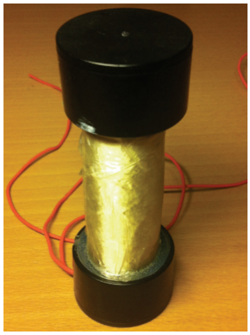

Figure 1: DEAP push transducer.

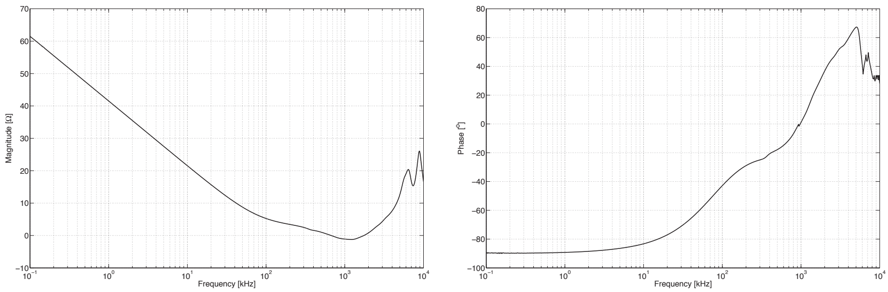

(a) Magnitude.

(b) Phase.

Figure 2: Measured impedance.

Theory

Due to the high series resistance of the DEAP transducer, the magnitude of the ripple current becomes a concern. Conduction losses will dominate, if the ripple current becomes to high. This is both a problem in terms of efficiency, but also because of the reduced lifetime of the contact interface. In order to estimate the switching frequency required for maintaining sufficiently low current ripple with second-order and fourth-order output filtering, respectively, consider the Fourier series representing of a pulse-width modulation signal (D = 0.5)

$$v_{PWM}(t) = \frac{4V_S}{\pi} sin(2\pi ft) + \frac{4V_S}{3\pi} sin(3 \cdot 2\pi ft) \tag{1}$$

$$\frac{4V_S}{5\pi} sin(5 \cdot 2\pi ft) + \ldots \tag{2}$$

Using fundamental component analysis it can be assumed that

$$v_{PWM}(t) \approx \frac{4V_S}{\pi} sin(2\pi ft) \tag{3}$$

The transfer function from input voltage to capacitor current for the second-order output filter is

$$\frac{i_C(s)}{v_{PWM}(s)} = \frac{C_{DEAP}s}{C_{DEAP}L_1 s^2 + \frac{L}{R}s + 1} \tag{4}$$

If a signal frequency is applied well above $\omega_0 = \frac{1}{\sqrt{L_1 C_{DEAP}}}$, equation (4) can be simplified to

$$\left| \frac{i_C(j\omega)}{v_{PWM}(j\omega)} \right|_{\omega \gg \omega_0} \cong \frac{1}{L_1 \omega} \tag{5}$$

The current ripple is found by multipling equation (3) with equation (8)

$$\Delta i_C = \frac{2V_S}{\pi^2 L f} \tag{6}$$

For the fourth-order output filter a similar approach can show that

$$\frac{i_C(s)}{v_{PWM}(s)} = \frac{C_{DEAP}s}{s^4 L_1 L_2 C_1 C_{DEAP} + s^3 \frac{L_1 L_2 C_1}{R} + s^2(L_1 C_{DEAP} + L_1 C_1 + L_2 C_{DEAP}) + s\frac{L_1+L_2}{R} + 1} \tag{7}$$

$$\left|\frac{i_C(j\omega)}{v_{PWM}(j\omega)}\right|_{\omega \gg \omega_0} \cong \frac{1}{L_1 L_2 C_1 \omega^3} \tag{8}$$

$$\Delta i_C = \frac{V_S}{2 L_1 L_2 C_2 \pi^4 f^3} \tag{9}$$

Consider a case study where $V_S = 300$ V, $L_1 = 200\mu H$ and $f_{Sw} = 285$ kHz, the current ripple through the DEAP transducer becomes $\Delta i_C = \frac{2 \cdot 300V}{200\mu H 2\pi 285kHz} = 1.59$ A peak for the 2th order output filter solution. Assuming $L_1 = L_2 = 200\mu H$ and $C_1 = 100nF$, $\Delta i_C = \frac{300V}{2 \cdot 200\mu H 200\mu H 100nF\pi^4(285kHz)^3} = 16.6$ mA peak for the 4th order output filter solution. With a worst case series resistance of 10 Ω, the 2th order output filter solution will yield a loss of 8.43 W, while the loss of the 4th order output filter solution is 0.92 mW. For an amplifier producing a maximum output power of 125 Var, the 4th order output filter solution becomes the right choice in terms of efficiency. A formal definition of the efficiency will be given later. Another benefit of the 4th order output filter solution is the possibility for a film capacitor to be used in the first LC-filter stage. The high frequency content will then flow through a capacitor with a frequency response much better than that of the DEAP transducer.

Control

Hysteresis based self-oscillating control schemes have received great interest in class D audio amplifiers due to the superior loop gain [11, 12, 13]. The switching frequency is defined as

$$f_{Sw}(D) = \frac{D(1-D)}{2\frac{V_{Hyst}}{K} + t_D} \tag{10}$$

With D been the duty cycle, t_D the control-loop delay, v_{Hyst} the height of the hysteresis window, and

$$K = 2V_S \times step\{\lim_{s\to\infty} G_{Ctrl}(s)\} \tag{11}$$

For the purpose of designing the self-oscillation control-loop, the controller transfer function must be defined as

$$G_{Ctrl}(s) = \frac{v_{Carrier}(s)}{v_{PWM}(s)} \tag{12}$$

$$= K_{Vfb_1}\frac{v_{C_1}(s)}{v_{PWM}(s)} + K_{Vfb_2}\frac{v_{Out}(s)}{v_{PWM}(s)} + K_{Cfb_1}\frac{i_{L_1}(s)}{v_{PWM}(s)} + K_{Cfb_2}\frac{i_{L_2}(s)}{v_{PWM}(s)} \tag{13}$$

where definitions from figure 3(a) is utilized.

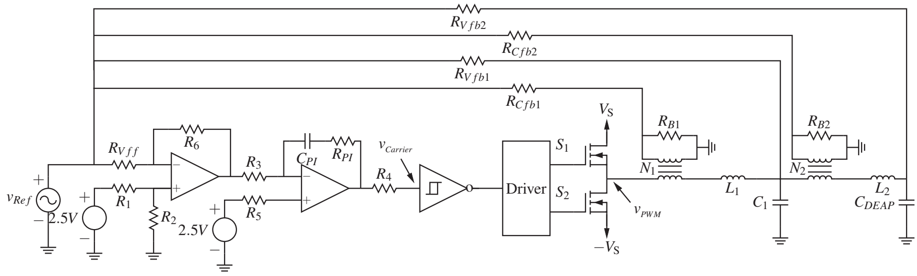

(a) Schematic with single-supply control circuitry.

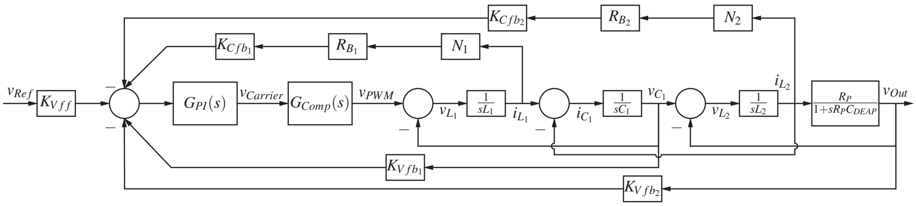

(b) Small-signal model.

Figure 3: Prototype class D amplifier with 4th order output filter and control.

Transfer functions

The transfer functions of equation (13) are defined as

$$\frac{v_{Out}(s)}{v_{PWM}(s)} = \frac{1}{s^4L_1L_2C_1C_2 + s^3\frac{L_2L_1C_1}{R_P} + s^2(C_1L_1 + L_2C_2 + L_1C_2) + s\frac{L1+L2}{R_P} + 1} \tag{14}$$

$$\frac{v_{C_1}(s)}{v_{PWM}(s)} = \frac{s^2L_2C_2 + s\frac{L_2}{R_P} + 1}{s^4L_1L_2C_1C_2 + s^3\frac{L_2L_1C_1}{R_P} + s^2(C_1L_1 + L_2C_2 + L_1C_2) + s\frac{L1+L2}{R_P} + 1} \tag{15}$$

$$\frac{i_{L_1}(s)}{v_{PWM}(s)} = \frac{s^4L_1L_2C_1C_2 + s^3\frac{L_2L_1C_1}{R_P} + s^2(C_1L_1 + L_1C_2) + s\frac{L1}{R_P}}{sL_1(s^4L_1L_2C_1C_2 + s^3\frac{L_2L_1C_1}{R_P} + s^2(C_1L_1 + L_2C_2 + L_1C_2) + s\frac{L1+L2}{R_P} + 1)} \tag{16}$$

$$\frac{i_{L_2}(s)}{v_{PWM}(s)} = \frac{s^2L_2C_2 + s\frac{L_2}{R_P}}{sL_2(s^4L_1L_2C_1C_2 + s^3\frac{L_2L_1C_1}{R_P} + s^2(C_1L_1 + L_2C_2 + L_1C_2) + s\frac{L1+L2}{R_P} + 1)} \tag{17}$$

The feedback coefficients defined in figure 3(b) are

$$K_{Vfb_1} = \frac{R_{Vfb2}||R_{Cfb1}||R_{Cfb2}||R_{Vff}}{R_{Vfb2}||R_{Cfb1}||R_{Cfb2}||R_{Vff} + R_{Vfb1}} \tag{18}$$

$$K_{Vfb_2} = \frac{R_{Vfb2}||R_{Cfb1}||R_{Cfb2}||R_{Vff}}{R_{Vfb2}||R_{Cfb1}||R_{Cfb2}||R_{Vff} + R_{Vfb2}} \tag{19}$$

$$K_{Cfb_1} = \frac{R_{Vfb2}||R_{Cfb1}||R_{Cfb2}||R_{Vff}}{R_{Vfb2}||R_{Cfb1}||R_{Cfb2}||R_{Vff} + R_{Cfb1}} \tag{20}$$

$$K_{Cfb_2} = \frac{R_{Vfb2}||R_{Cfb1}||R_{Cfb2}||R_{Vff}}{R_{Vfb2}||R_{Cfb1}||R_{Cfb2}||R_{Vff}+R_{Cfb2}} \quad (21)$$

$$K_{Vff} = \frac{R_{Vfb2}||R_{Cfb1}||R_{Cfb2}||R_{Vff}}{R_{Vfb2}||R_{Cfb1}||R_{Cfb2}||R_{Vff}+R_{Vff}} \quad (22)$$

Design

Using equation (13) and equation (11), the constant K can be derived

$$K = \frac{2V_s K_{Cfb_1} N_1 R_{B_1}}{L_1} \quad (23)$$

It is assumed, that the inner current loop is dominating at the high frequencies.

Experimental results:

A $\pm$ 300 V half-bridge based class D amplifier driving a 100 nF load in the midrange region of 0.1-3.5 kHz is used for experimental verification. The amplifier is build around a Si8235 isolated gate driver and SPA08N80C3 MOSFET's. Figure 4(a) shows a picture of the prototype amplifier. Design parameters are presented in Table I, while derived component values are gathered in Table II.

Efficiency

When driving a DEAP transducer it is appropriate to give a formal definition of the term efficiency. The first order approximation will yield a capacitive load. Accordingly no real power will be delivered to the load. Efficiency will thus be defined as

$$\eta = \frac{P_{Out}}{P_{Out}+P_{In}} \quad (24)$$

where $P_{Out} = \frac{V_{rms}^2}{\left(\frac{1}{2\pi f_{Ref} C_{Deap}}\right)}$, is the reactive power delivered to the load, and P_{In} corresponds to the real power consumed by the amplifier. This definition of the term efficiency will be used throughout the paper.

The measured efficiency can be seen in figure 4(b). The efficiency is defined in accordance with equation 24. Note, that the efficiency at 100 Hz is below 40 %. Because the output voltage is kept fixed with respect to frequency, the reactive output power will drop inversely proportional with the frequency. At 100 Hz the switching loss becomes comparable with the reactive output power. An efficiency above 80 % is achieved for the frequencies of 1 and 3.5 kHz. Voltage mode control of electrostatic transducers is preferred for applications where displacement is of concern. Charge mode control ensures greater linearity at the expense of displacement [14].

	Designator	Value
Idle switching frequency	f_{Sw}	285 kHz
Output filter inductance	L_1	200 uH
Output filter inductance	L_2	200 uH
Output filter capacitance	C_1	100 nF
DEAP Capacitance	C_{DEAP}	100 nF
Supply voltage	$\pm V_S$	$\pm 300V$
Closed loop gain	A_V	75 $\frac{V}{V}$

Table I: Design parameters.

Component	Value
R_{B_1}	110 Ω
R_{B_2}	10 Ω
C_{PI}	1.5 nF
R_{PI}	1 $k\Omega$
R_{Cbf_1}	4 $k\Omega$
R_{Cbf_2}	4 $k\Omega$
R_{Vff}	2 $k\Omega$
R_{Vfb_1}	300 $k\Omega$
R_{Vfb_2}	300 $k\Omega$
R_1, R_2, R_3, R_4, R_5 and R_6	1 $k\Omega$
N_1 and N_2	$\sqrt{\frac{200nH}{980uH}} \approx 0.014$

Table II: Component values.

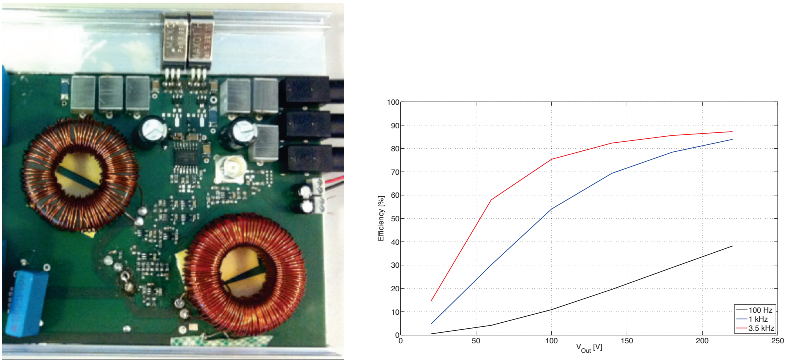

(a) Picture of prototype amplifier.

(b) Efficiency.

Figure 4: Prototype amplifier.

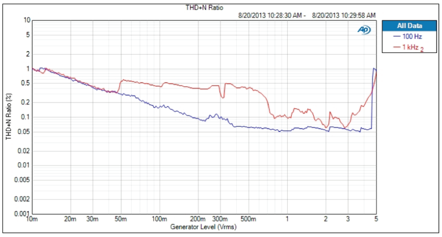

Figure 5: THD+N of the prototype for reference frequencies of 100 Hz and 1 kHz.

THD+N

THD+N is measured using an APX525 audio analyzer and a voltage attenuation interface. The voltage attenuation interface is necessary in order to protect the input-stage of the audio analyzer. Design and implementation of the voltage attenuation interface is well-described in the literature [10, 15]. Figure 5 gives the measured THD+N as a function of the reference voltage for the frequencies of 100 Hz and 1 kHz. THD+N is below 0.1% over a significant part of the operation range for the reference frequency of 100 Hz. Noise is the dominating factor in the measured THD+N.

Conclusion:

A class D audio amplifier with 4th order output filter for capacitive transducers is proposed and analyzed. The amplifier addresses the issues of high series resistance and limited frequency response of the capacitive transducers, potentially paving the way for increased industry adoption of this highly promising technology. THD+N below 0.1% is reported for the ± 300 V prototype amplifier producing a maximum of 125 Var at a peak efficiency of 87 %.

References

[1] K. Nielsen, “Audio power amplifier techniques with energy efficient power conversion,” Ph.D. dissertation, Technical University of Denmark, 1998.

[2] S. Poulsen, “Towards active transducers,” Ph.D. dissertation, Technical University of Denmark, July 2004.

[3] S. Poulsen and M. A. E. Andersen, “Hysteresis controller with constant switching frequency,” *Consumer Electronics, IEEE Transactions on*, vol. 51, no. 2, pp. 688–693, 2005.

[4] S. Poulsen and M. A. E. Andersen, “Simple pwm modulator topology with excellent dynamic behavior,” in *Applied Power Electronics Conference and Exposition, 2004. APEC’04. Nineteenth Annual IEEE*, vol. 1. IEEE, 2004, pp. 486–492.

[5] S. Poulsen and M. A. Andersen, "Practical considerations for integrating switch mode audio amplifiers and loudspeakers for a higher power efficiency," in *Audio Engineering Society Convention 116*, 2004.

[6] R. Sarban, R. Jones, B. Mace, and E. Rustighi, "A tubular dielectric elastomer actuator: Fabrication, characterization and active vibration isolation," *Mechanical Systems and Signal Processing*, vol. 25, no. 8, pp. 2879–2891, 2011.

[7] R. Heydt, R. Kornbluh, R. Pelrine, and V. Mason, "Design and performance of an electrostrictive-polymer-film acoustic actuator," *Journal of Sound and Vibration*, vol. 215, no. 2, pp. 297–311, Aug. 1998.

[8] R. Heydt, R. Pelrine, J. Joseph, J. Eckerle, and R. Kornbluh, "Acoustical performance of an electrostrictive polymer film loudspeaker," *Journal of the Acoustical Society of America*, vol. 107, no. 2, pp. 833–839, Feb. 2000.

[9] D. Nielsen, A. Knott, and M. A. E. Andersen, "Hysteretic self-oscillating bandpass current mode control for class d audio amplifiers driving capacitive transducers," 2013.

[10] D. Nielsen, A. Knott, and M. A. E. Andersen, "Driving capacitive transducers," in *Audio Engineering Society*, 134th Convention, Ed. Rome, Italy, 2013.

[11] M. C. Høyerby and M. A. Andersen, "Derivation and analysis of a low-cost, high-performance analogue bpcm control scheme for class-d audio power amplifiers," in *Audio Engineering Society Conference: 27th International Conference: Efficient Audio Power Amplification*, 2005.

[12] M. C. W. Hoyerby and M. A. E. Andersen, "Carrier distortion in hysteretic self-oscillating class-d audio power amplifiers: Analysis and optimization," *IEEE Transactions On Power Electronics*, vol. 24, no. 3-4, pp. 714–729, Mar-Apr 2009.

[13] M. Høyerby and M. Andersen, "A small-signal model of the hysteretic comparator in linear-carrier self-oscillating switch-mode controllers," *Norpie*, 2006.

[14] J. Borwick, *Loudspeaker and Headphone Handbook*, third edition ed. Reed Educational and Professional Publishing Ltd, 2001, no. 0 240 51578 1.

[15] A. P. Inc., "Measuring high impedance sources," *http://ap.com/kb/show/314*, 2010.